Oceanological and Hydrobiological Studies

International Journal of Oceanography and Hydrobiology

Volume 49, No. 4, December 2020
pages (398-407)

ISSN 1730-413X
eISSN 1897-3191

Seasonal and annual variability in chlorophyll-*a* in the shelf region of the Northern Bay of Bengal using MODIS-Aqua data

by

Muhammad Abdur Rouf*,
Al-Hasan Antu,
Md. Imran Noor

DOI: **10.1515/ohs-2020-0035**
Category: **Original research paper**
Received: **January 7, 2020**
Accepted: **April 24, 2020**

Fisheries & Marine Resource Technology Discipline, Khulna University, Khulna, Bangladesh

Abstract

Chlorophyll-*a* (Chl-*a*) concentration is an important issue in ocean ecosystem management and research. This study investigates seasonal and annual variability in Chl-*a* and its relationship with sea surface temperature (SST) and river discharge in the shelf region of the Northern Bay of Bengal (BoB), as well as validates satellite data against in-situ data. Moderate Resolution Imaging Spectroradiometer (MODIS) Aqua satellite data on Chl-*a* concentration and SST from 2002–2018 were used in this study. River discharge data were obtained from the Bangladesh Water Development Board (BWDB). The annual Chl-*a* concentration ranged from 2.08 to 2.94 mg m^{-3}, with an average of 2.43 ± 0.24 mg m^{-3}. The Chl-*a* concentration was found higher (2.21 ± 0.56 mg m^{-3}) during the northeast monsoon (October–February) and lower (1.81 ± 1.14 mg m^{-3}) during the pre-monsoon season (March–May). The study revealed a declining trend in Chl-*a* concentration from 2002 to 2018, and the rate of change was –0.0183 mg m^{-3} $year^{-1}$. Chl-*a* concentration showed a weak inverse relationship with SST, both annually and seasonally, especially in the pre-monsoon season. River discharge masked the effect of SST on Chl-*a* variability during the southwest and northeast monsoon. A reasonable correlation (r = 0.78) was found between the MODIS-Aqua data and in-situ Chl-*a* observations.

Key words: Chlorophyll-*a*, seasonal variability, annual variability, MODIS, continental shelf, Bay of Bengal, Bangladesh

* Corresponding author: roufku@yahoo.com

DE GRUYTER

online at www.oandhs.ug.edu.pl

Introduction

Chlorophyll-*a* (Chl-*a*) is the main pigment used by phytoplankton in photosynthesis to convert nutrients and carbon dioxide. The distribution of Chl-*a* in the ocean indicates the biophysical quality of water and the abundance of biological resources. Therefore, Chl-*a* has an important impact on marine fishery resources and their development in the coastal marine environment (Radiarta & Saitoh 2008). Chl-*a* distribution has been studied in various regions of the world ocean (Shetye et al. 1996; Sarangi et al. 2008; Singh & Chaturvedi 2010; Brewin et al. 2013; Zhang et al. 2017). However, it has not been studied in the shelf region of Bangladesh, which could be used to achieve the targets under the component (Goal 14: Life below water) of the Sustainable Development Goals (SDG) after the recent settlement of maritime border disputes.

A considerable understanding of temporal dynamics of biophysical factors describing coastal water systems is required to appropriately manage and monitor valuable coastal ecosystems. For this purpose, remote sensing could be an effective tool. High resolution, multispectral satellite data have been used in recent decades to detect regular chemical, biological, and physical phenomena in coastal waters. Nonetheless, monitoring of coastal waters using the existing satellite instruments is a challenging task and requires extremely sophisticated procedures (Chauhan et al. 2002).

Spatial ocean parameters, such as Chl-*a,* have been extensively studied using time series of satellite data derived from ocean color satellite measurements. The MODIS-Aqua satellite sensor is one of the most popular satellites providing data for the ocean. It is monitored by the National Aeronautics and Space Administration (NASA) and is popular among ocean dynamics researchers (Singh & Chaturvedi 2010).

Several efforts have been made to study Chl-*a* variability in the Arabian Sea, which is adjacent to the Bay of Bengal (BoB; Sathyendranath et al. 1991; Bhattathiri et al. 1996). Although some studies discuss the Chl-*a* distribution in the BoB, most of them are based on the southwestern and western parts of BoB (Prasad & Singh 2010; Nagamani et al. 2011; Nagamani et al. 2013; Poornima et al. 2013; Suwannathatsa & Wongwises 2013). Thus, no studies were found that would focus particularly on the shelf region of the northern part of the BoB. Therefore, we took the first step toward understanding the variability of Chl-*a* concentration in this region.

The shelf region of Bangladesh is relatively flat without being cut-off by a submarine canyon and extends for approximately 150–200 km with a depth of 150–200 m (Qasim 1977). The region is unique due to an enormous freshwater flux from surrounding rivers and seasonally reversed monsoon winds, and exerts a strong impact on the surface water circulation and stratification (Sarangi et al. 2008). During monsoons, large volumes of freshwater discharged by the Ganga-Brahmaputra-Meghna rivers significantly reduce the salinity and intensity of upwelling at a distance of up to ~40 km from the coast (Shetye et al. 1996). Therefore, the monsoon and river discharge may affect the Chl-*a* distribution in the shelf region. In general, the sea surface temperature (SST) has an inverse relation with Chl-*a* distribution and the trend in this relation is consistent mainly in the offshore region, but not always in the shelf region (Khalil et al. 2009). Thus, a baseline study is required.

This study, therefore, aimed to investigate annual and seasonal variability in Chl-*a* and its relationship with SST and river discharge in the shelf region of the northern BoB and validates the MODIS-Aqua satellite data against in-situ data.

Materials and methods

The study focused on the shelf region of the northern BoB (latitude: from 20°N to 23°N; longitude: from 88.77°E to 92.70°E), which extends up to a depth of 200 m (Fig. 1).

Chl-*a*, SST, and river discharge data were considered in this study. MODIS-Aqua Level 3 mapped 4 km resolution monthly and annual Chl-*a* concentration and SST data for 2002–2018 were retrieved from the Ocean Biology Distributed Active

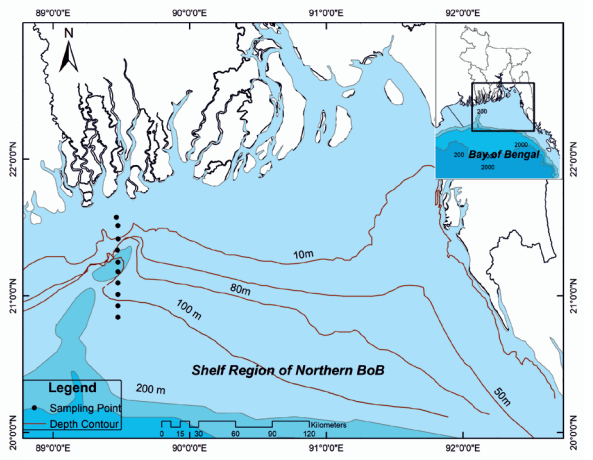

Figure 1

Shelf region of the northern BoB including 10 sampling locations

Archive Center (OB. DAAC) of NASA (https://oceancolor.gsfc.nasa.gov/l3/).

MODIS-Aqua Chl-*a* data use the OCI (Ocean Color Index) algorithm to derive Chl-*a* values from the recorded radiance. The OCI algorithm is a combination of two algorithms, the O'Reilly band ratio OCx (chl_oc4) algorithm (O'Reilly et al. 1998) and the Hu color index (CI) algorithm (Hu et al. 2012).

The SST data are generated using both 11 and 12 µm long wave infrared bands. The current SST algorithm is based on a modified version of the nonlinear SST algorithm of Walton et al. (1998). It is applicable to the MODIS sensor for both daytime and nighttime observations. In this study, daytime 11 µm data were used to analyze the SST values. The MODIS Aqua monthly and annual-scale Chl-*a* and SST datasets were processed and analyzed using SeaDAS 7.4.

River discharge data (2002–2018) were obtained from the Bangladesh Water Development Board (BWDB). River discharge data from two stations (SW273 and SW93.5L), which cover the major discharge into the BoB, were used to determine the impact of inland discharge on Chl-*a* concentration.

For in-situ measurements, the United Nations Educational, Scientific and Cultural Organization (UNESCO) monograph (Jeffrey & Mantoura 1997) was followed. Aminot & Rey (2001) was also followed for adequate quality assessment and quality control practices. The in-situ Chl-*a* determination was based on 90% acetone extraction. Water samples were collected from ten sampling locations covering a latitude of 21°34′28.8″N to 20°50′37.0″N and a longitude of 89°28′E, with a 5′ (5 min) geographical coordinate interval (Fig. 1). Water sampling dates for this study were 12 and 13 November 2017, 2 December 2017 and 7 January 2018 during daytime. A nitrocellulose filter of 47 mm diameter and 0.45 µm pore size was used in the filtration process. The extract volume was maintained at 10 ml of 90% acetone (i.e. 10 ml + dead volume of the filter). The absorbance of sample extracts was measured at 750 nm and 665 nm in a Hitachi U-2910 spectrophotometer against 90% acetone blank before and after acidification with 2 drops of 1N HCl. The absorbance readings obtained at 665 nm and 750 nm before and after acidification and cell to cell differences were entered in the following monochromatic equation of Lorenzen (1967), which is recommended for Chl-*a* estimation in coastal and estuarine waters:

$$\text{chl-}a\ (\text{mg m}^{-3}) = \frac{A \times K \times [(E_{665o} - E_{750o}) - (E_{665a} - E_{750a})] \times V_e}{L \times V_f}$$

where:

A = absorption coefficient of chl-*a* (11.4 µg cm ml^{-1})
L = cuvette light-path in centimeter (cm)
V_e = extraction volume in milliliter (ml)
V_f = filtered volume in liter (l)
E_{665o} and E_{750o} = absorbance of 665 nm and 750 nm, respectively, before acidification
E_{665a} and E_{750a} = absorbance of 665 nm and 750 nm, respectively, after acidification
R = maximum absorbance ratio of E_{665o}/E_{665a} in the absence of pheopigments (1.7)
K = R / (R – 1) = 2.43

Results and discussion

Annual trend in Chl-*a* concentration

The annual time series data (2002–2018) acquired from the MODIS-Aqua satellite revealed a complex variability in Chl-*a* concentration in the shelf region of the northern BoB. The maximum and minimum annual average Chl-*a* concentration in the study area was 2.94 mg m^{-3} in 2004 and 2.08 mg m^{-3} in 2015, respectively. The annual chronological Chl-*a* satellite images from 2002 to 2018 are shown in Figure 2. Considering the spatial variability, we found a higher and wider range of Chl-*a* concentration (0.18–15.93 mg m^{-3}) in the study area compared with other studies that were performed in the western (0.1–0.9 mg m^{-3}; Nagamani et al. 2011) and southwestern (0.1–2.0 mg m^{-3}; Sarangi et al. 2008) region of the BoB. The high Chl-*a* concentration is caused by the river discharge along the coast (Dasgupta et al. 2009) with a depth of 200 m combined with strong winds (Dey & Singh 2003; Patti et al. 2008; Dasgupta et al. 2009; Singh & Chaturvedi 2010).

Annual variations are generally influenced by physical properties (temperature, salinity, and dissolved inorganic nutrient concentration) of the ocean. Different regions of the ocean generally show different patterns of Chl-*a* concentration, which are affected by diverse factors, such as tidal effects, inconsistent upwelling and long-term environmental changes (i.e. SST). Upwelling can be an important factor affecting long-term changes in Chl-*a* concentration. In our study, the annual Chl-*a* concentration in the shelf region of the BoB showed a declining trend between 2002 and 2018, which follows a simple linear regression with a rate of –0.0183 mg m^{-3} yr^{-1} (Fig. 3). Behrenfeld et al. (2006) found a declining trend in Chl-*a* concentration over nine years and attributed it to several climatic factors, particularly SST, and some local factors. A similar finding was reported by Brodie et al. (2007).

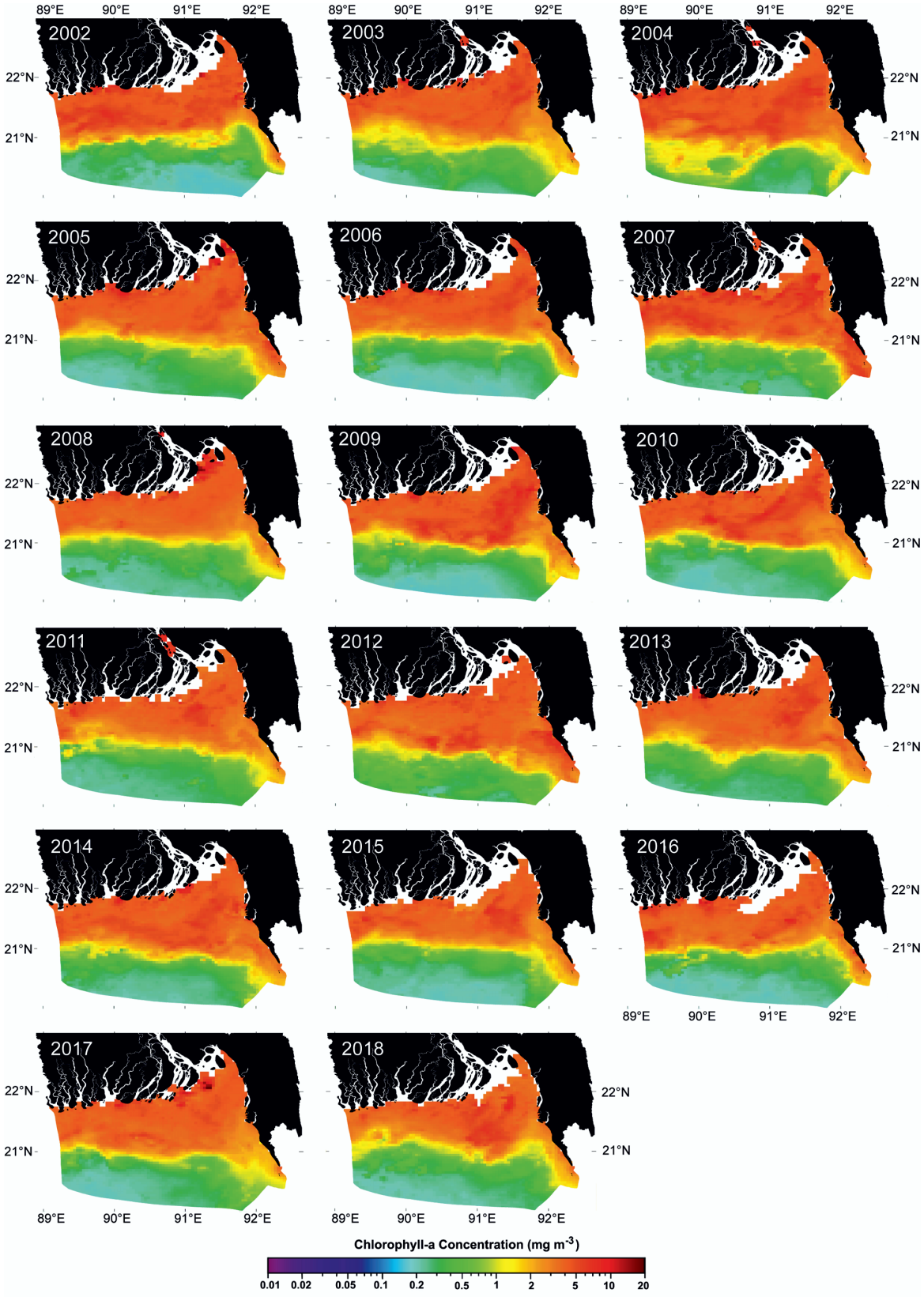

Figure 2

MODIS-Aqua satellite-derived annual composite Chl-*a* concentration images from 2002 to 2018

Seasonal trend in Chl-*a* concentration

Chl-*a* concentration was higher (2.21 ± 0.56 mg m^{-3}) during the northeast monsoon (October–February), within the range of 0.20–4.85 mg m^{-3}, and lower (1.81±1.14 mg m^{-3}) during the pre-monsoon (March–May), within the range of 0.27–5.94 mg m^{-3} (Fig. 4). The seasonal pattern of Chl-*a* concentration in the shelf region of the BoB is illustrated with monthly

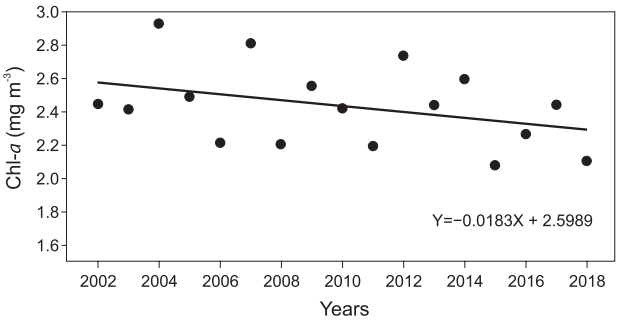

Figure 3

Annual trend in Chl-*a* concentration from 2002 to 2018

climatological composites of the MODIS-Aqua images from July 2002 to June 2018 (Fig. 5). Figures 4 and 5 clearly show that Chl-*a* concentration gradually increased from the end of the southwest monsoon (September), was mostly high during the northeast monsoon (October–February), and relatively low in pre-monsoon (March–May).

The relatively high concentration of Chl-*a* (2.21 ± 0.56 mg m^{-3}) in the northeast season represents a highly productive season. The high Chl-*a* concentration in this season is associated with run-off from the main rivers, low SST (~26°C), and coastal plumes (Chaturvedi 2005; Sarangi et al. 2008; Nagamani et al. 2011). Of the northeast season months, October and November showed higher

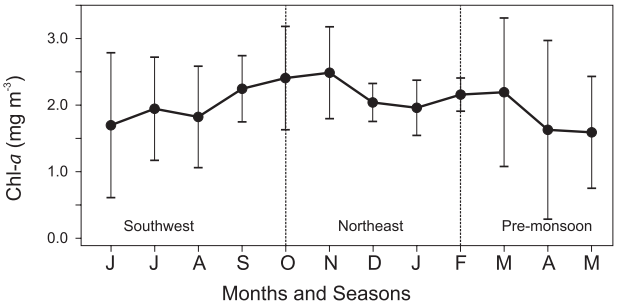

Figure 4

Seasonal trend in Chl-*a* concentration (July 2002 to June 2018)

Chl-*a* concentration (2.41 mg m^{-3} and 2.49 mg m^{-3}, respectively). A higher river discharge (7578.55 m^3 s^{-1}) was observed in this region in July–September, whereas high Chl-*a* concentration was observed in September–November, thus indicating a lag time. This time lag was mainly caused by the time required for the ocean to respond to the wind, forcing the nutrient-rich water to reach the surface for the phytoplankton cells to grow (Sarangi & Devi 2017). Suwannathatsa & Wongwises (2013) also found high Chl-*a* concentration (5–15 mg m^{-3}) along the coasts of Bangladesh from late October to January due to strong currents and river run-off. Several cyclones occur in the BoB in October–December, which provide the surface with nutrient-rich subsurface water, form eddies and intensify blooms, and consequently play a role in the formation of high Chl-*a* concentration (Chauhan et al. 2002; Madhu et al. 2002; Sarangi et al. 2008). Sarangi & Devi (2017) reported the maximum number of larger eddies, observed particularly in October, and indicated the eddy pumping as a possible mechanism of vertical transfer of nutrients across the halocline to the oligotrophic or eutrophic zone in the BoB. A similar observation was made by Bhushan et al. (2018), Krishna (2013), and Venkateswrlu & Rao (2004) in connection with a cyclonic disturbance. Nagamani et al. (2011) also observed dense Chl-*a* patches (~1.0 mg m^{-3}) after a cyclone in the BoB in October 1999. Thus, the BoB receives much attention in regard to Chl-*a* due to the formation of severe tropical cyclones.

The lowest Chl-*a* concentration was found in the shelf region of the northern BoB during the pre-monsoon season (March–May). It occurred due to a gradual increase in SST (detailed relationship between Chl-*a* concentration and SST are described in the subsequent section) and a decrease in wind speed (Nagamani et al. 2013). The compensation of the northeast and southwest monsoons during the transition period from winter to summer neutralizes the propagated strong currents (Suwannathatsa & Wongwises 2013), which explains the decrease in Chl-*a* concentration to the lowest level in the year.

Relationship between Chl-*a* concentration and SST

The seasonal trend in Chl-*a* concentration and SST is shown in Figure 6 and the statistical relations are shown in Table 1. The linear regression analysis showed a weak inverse relation between the annual Chl-*a* concentration and SST. The inverse relationship between the Chl-*a* concentration and SST was found only during the pre-monsoon, while a positive relation was found during the northeast and southwest monsoon.

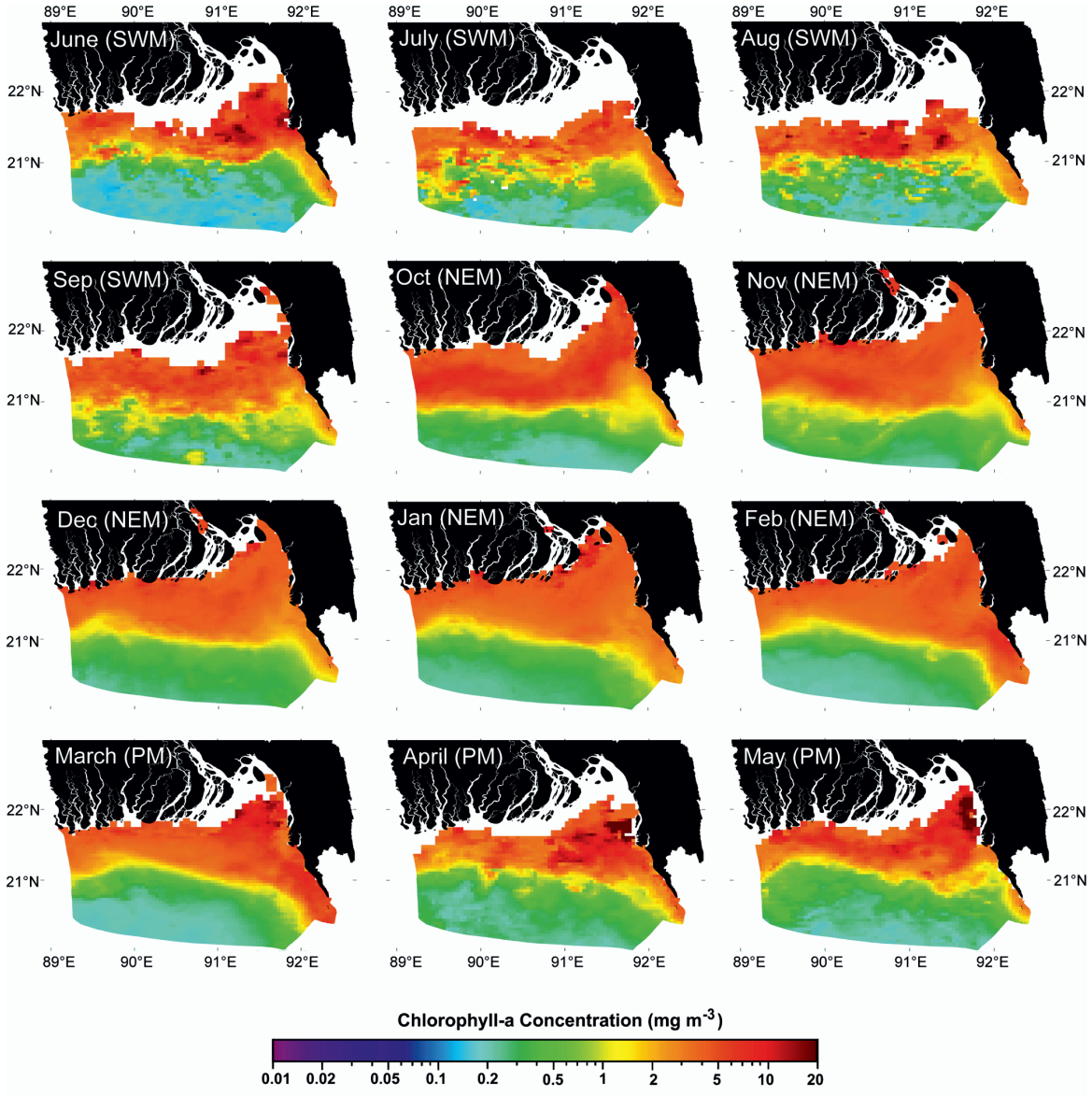

Figure 5

MODIS-Aqua-derived monthly climatological Chl-*a* concentration images from July 2002 to June 2018 (SWM – southwest monsoon, NEM – northeast monsoon, PM – pre-monsoon)

The positive relation (coefficient of regression, b = 0.254) during the southwest monsoon (June–September) contradicts the usual inverse relation between Chl-*a* concentration and SST. Rainfall and the associated freshwater intrusion through the adjacent rivers provide the onshore region of the BoB with nutrient-rich (nitrate, silicon, and phosphate) freshwater containing nitrate concentration patches in June–August (Sarangi & Devi 2017). This nitrate concentration (influx water nutrient) was associated more with Chl-*a* concentration than SST, as nitrate inherently enhances the ocean Chl-*a* (Sarangi & Devi 2017). Therefore, the freshwater influx masked the effect of SST on the Chl-*a* concentration variability in this season.

A positive relation (b = 0.070) was also observed during the northeast monsoon (October–February) between Chl-*a* concentration and SST. In this season, the shelf region of the BoB was exposed to a relatively smaller amount of the river discharge than the southwest monsoon (Sarangi et al. 2008; Nagamani et al. 2011; Sarangi & Devi 2017). Thus, a lower b-value was observed in this season compared to the southwest monsoon. During the pre-monsoon (March–May), an

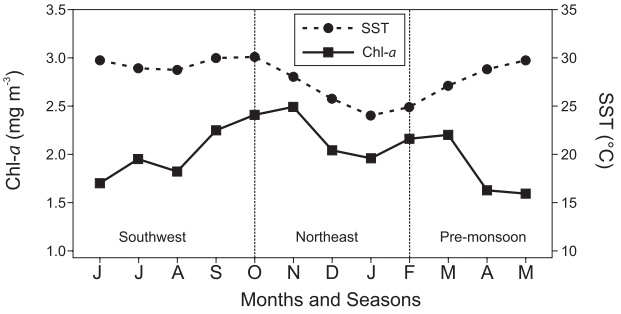

Figure 6

Seasonal trend in Chl-*a* concentration and SST

Table 1

Statistical analysis of Chl-*a* concentration and SST

Time Series	*a*	*b*	*r*	R^2	n
Southwest (June–September)	−5.505	0.254	0.224	0.050	61
Northeast (October–February)	0.345	0.070	0.283	0.080	80
Pre-monsoon (March–May)	6.604	−0.168	−0.186	0.035	47
Annual data (2002–2018)	8.951	−0.237	−0.326	0.160	17

inverse relation (b = −0.168) was observed between Chl-*a* concentration and SST. In this season, the river discharge rate was insignificant due to lower rainfall. Therefore, the impact of the river discharge on Chl-*a* concentration was extremely low, indicating that the river discharge did not mask the effect of SST in this season, as opposed to the southwest and northeast monsoon.

An inverse (b = −0.237) relation (Table 1) was also found between the annual Chl-*a* concentration and SST (Fig. 7). This inverse relationship was relatively weaker than in most scientific researches (Smyth et al. 2001; Behrenfeld et al. 2006; Brodie et al. 2007), which allowed us to conclude that SST has a weak relation with Chl-*a* concentration in the shelf region of the northern BoB.

Relationship between Chl-*a* concentration and river discharge

The average annual river discharge between 2002 and 2018 was 6923 ± 915.37 $m^3 s^{-1}$. The highest amount of discharge was 9154 $m^3 s^{-1}$ in 2002, whereas the lowest amount was 5723 $m^3 s^{-1}$ in 2009. The higher amount of the river discharge was observed during the southwest monsoon (June–September) and it ranged from 4425 to 13329 $m^3 s^{-1}$ with an average of 7579 $m^3 s^{-1}$.

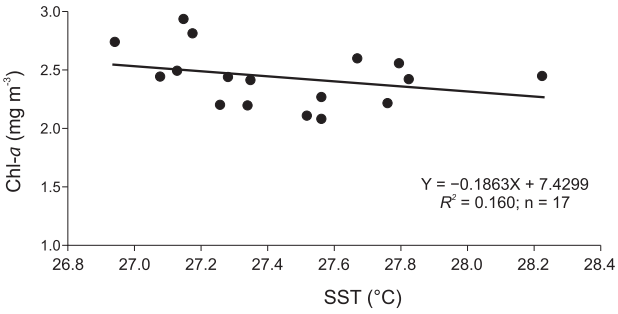

Figure 7

Annual relationship between Chl-*a* concentration and SST

The Chl-*a* concentration and river discharge showed a positive relation (b = 0.004, R^2 = 0.25, n = 17; Fig. 8). This positive relation is mostly due to the Ganga delta, which is the largest delta in the world (Coleman 1969; Kuehl et al. 1997; Goodbred et al. 2003), carrying anthropogenic deposits from thousands of kilometers of riverside settlements (Goodbred & Kuehl 2000; Islam & Gnauck 2008). The coefficient of determination (R^2 = 0.25, n = 17) between Chl-*a* concentration and river discharge obtained in this study was relatively higher than the coefficient of determination (R^2 = 0.16, n = 17) between Chl-*a* concentration and SST (see Table 1), which implies that the river discharge has a greater impact on Chl-*a* concentration than SST. Scholars agree that the river discharge has a greater effect on Chl-*a* concentration than other factors, e.g. upwelling, weather pattern, wind direction, floods, chemical compositions of water, biological parameters, geographical location, climatic factors (Johnson et al. 1999; Barnett et al. 2001; Levitus et al. 2001; Behrenfeld et al. 2006; Brodie et al. 2007; Subramaniam et al. 2008). Therefore, it is evident that the river discharge is one of the main driving factors affecting the variability of Chl-*a* concentration in the study area.

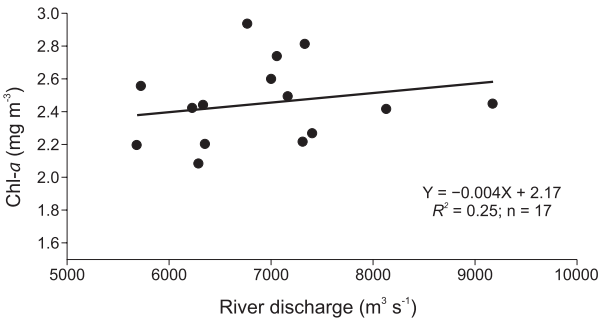

Figure 8

Relationship between Chl-*a* concentration and river discharge

Validation of satellite measurements by in-situ measurements

The correlation coefficient between the in-situ values and MODIS-Aqua satellite-derived Chl-*a* concentration was 0.78 (n = 120) with the R^2 value of 0.70 (Fig. 9). Nagamani et al. (2013) observed a high correlation coefficient of 0.842 between the in-situ and satellite data in the coastal water of the BoB. Haëntjens et al. (2017) also found an R^2 value of approximately 0.67 for the southern ocean, while compared the in-situ Chl-*a* concentration data with MODIS Aqua satellite Chl-*a* concentration data using the OCI algorithm.

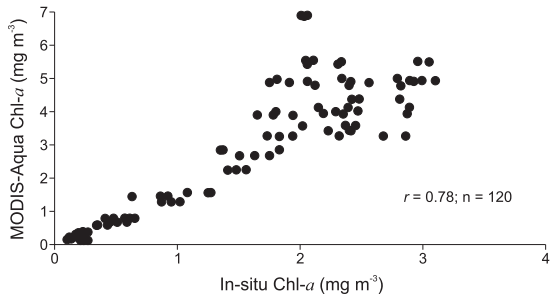

Figure 9

Correlation between in-situ and MODIS Aqua satellite

Conclusions

This study presents the seasonal and annual variability in Chl-*a* concentration and its relationship with SST and river discharge in the shelf region of the northern BoB using MODIS-Aqua satellite data. A decrease in Chl-*a* concentration was observed between 2002 and 2018. The highest Chl-*a* concentration was observed during the northeast monsoon season and the lowest in the pre-monsoon season. Chl-*a* concentration showed a weak inverse relation with SST, both annually and seasonally, especially in the pre-monsoon season. In this region, the river discharge mainly affected the Chl-*a* concentration variability during the southwest and northeast monsoon. Thus, monsoon has a significant effect on Chl-*a* concentration variability. In addition, various parameters (nitrate, phosphate, silicon, wind speed, cyclones, and eddies) also affect the Chl-*a* variability in coastal water, which was not covered by this study. Though we performed the in-situ measurements to validate the MODIS data, further extensive studies are needed to ensure the reliability of MODIS-Aqua data through a regional correction or inversion algorithm.

Acknowledgements

The authors are grateful to the Bangladesh Navy for helping to collect water samples from the northern BoB. The authors would also like to thank NASA's Ocean Biology Distributed Active Archive Center for MODIS-Aqua chlorophyll-*a* and SST data and the Bangladesh Water Development Board for providing river discharge data. Futhermore, the authors acknowledge the Khulna University Research Cell and the National Science and Technology (NST) fellowship of Bangladesh, which provided fincancial support for the research.

References

Aminot, A. & Rey, F. (2001). Chlorophyll *a*: Determination by spectroscopic methods. *ICES Tech. Mar. Environ. Sci.* 30(58): 17pp. DOI: 10.25607/OBP-278.

Barnett, T.P., Pierce, D.W. & Schnur, R. (2001). Detection of anthropogenic climate change in the world's oceans. *Science* 292(5515): 270–274. DOI: 10.1126/science.1058304.

Behrenfeld, M.J., O'Malley, R.T., Siegel, D.A., McClain, C.R., Sarmiento, J.L. et al. (2006). Climate-driven trends in contemporary ocean productivity. *Nature* 444(7120): 752–755. DOI: 10.1038/nature05317.

Bhattathiri, P., Pant, A., Sawant, S., Gauns, M., Matondkar, S. et al. (1996). Phytoplankton production and chlorophyll distribution in the eastarn and central Arabian Sea in 1994–1995. *Curr. Sci.* 71(11): 857–862. URL: http://drs.nio.org/drs/handle/2264/2149.

Bhushan, R., Bikkina, S., Chatterjee, J., Singh, S.P., Goswami, V. et al. (2018). Evidence for enhanced chlorophyll-a levels in the Bay of Bengal during early north-east monsoon. *J. Oceanogr. Mar. Sci.* 9(2): 15–23. DOI: 10.5897/JOMS2017.0144.

Brewin, R.J., Raitsos, D.E., Pradhan, Y. & Hoteit, I. (2013). Comparison of chlorophyll in the Red Sea derived from MODIS-Aqua and in vivo fluorescence. *Remote Sens. Environ.* 136: 218–224. DOI: 10.1016/j.rse.2013.04.018.

Brodie, J., De'ath, G., Devlin, M., Furnas, M. & Wright, M. (2007). Spatial and temporal patterns of near-surface chlorophyll a in the Great Barrier Reef lagoon. *Mar. Freshwater Res.* 58(4): 342–353. DOI: 10.1071/mf06236.

Chaturvedi, N. (2005). Variability of chlorophyll concentration in the Arabian Sea and Bay of Bengal as observed from SeaWiFS data from 1997–2000 and its interrelationship with Sea Surface Temperature (SST) derived from NOAA AVHRR. *Int. J. Remote Sens.* 26(17): 3695–3706. DOI: 10.1080/01431160500159818.

Chauhan, P., Mohan, M., Sarngi, R.K., Kumari, B., Nayak, S. et al. (2002). Surface chlorophyll a estimation in the

Arabian Sea using IRS-P4 Ocean Colour Monitor (OCM) satellite data. *Int. J. Remote Sens.* 23(8): 1663–1676. DOI: 10.1080/01431160110075866.

Coleman, J.M. (1969). Brahmaputra River: channel processes and sedimentation. *Sediment. Geol.* 3(2–3), 129–239. DOI: 10.1016/0037-0738(69)90010-4.

Dasgupta, S., Singh, R.P., & Kafatos, M. (2009). Comparison of global chlorophyll concentrations using MODIS data. *Adv. Space Res.* 43(7): 1090–1100. DOI: 10.1016/j.asr.2008.11.009.

Dey, S., & Singh, R.P. (2003). Comparison of chlorophyll distributions in the northeastern Arabian Sea and southern Bay of Bengal using IRS-P4 Ocean Color Monitor data. *Remote Sens. Environ.* 85(4): 424–428. DOI: 10.1016/s0034-4257(03)00025-7.

Goodbred S.L. & Kuehl, S.A. (2000). The significance of large sediment supply, active tectonism, and eustasy on margin sequence development: Late Quaternary stratigraphy and evolution of the Ganges–Brahmaputra delta. *Sediment. Geol.* 133(3–4), 227–248. DOI: 10.1016/s0037-0738(00)00041-5.

Goodbred S.L., Kuehl, S.A., Steckler, M.S., & Sarker, M.H. (2003). Controls on facies distribution and stratigraphic preservation in the Ganges–Brahmaputra delta sequence. *Sediment. Geol.* 155(3–4): 301–316. DOI: 10.1016/s0037-0738(02)00184-7.

Haëntjens, N., Boss, E. & Talley, L.D. (2017). Revisiting Ocean Color algorithms for chlorophyll a and particulate organic carbon in the Southern Ocean using biogeochemical floats. *J. Geophys. Res.: Oceans* 122(8): 6583–6593. DOI: 10.1002/2017JC012844.

Hu, C., Lee, Z. & Franz, B. (2012). Chlorophyll aalgorithms for oligotrophic oceans: A novel approach based on three-band reflectance difference. *J. Geophys. Res.: Oceans* 117(C1): C01011. DOI: 10.1029/2011jc007395.

Islam, S.N. & Gnauck, A. (2008). Mangrove wetland ecosystems in Ganges-Brahmaputra delta in Bangladesh. *Front. Earth Sci. China* 2(4): 439–448. DOI: 10.1007/s11707-008-0049-2.

Jeffrey, S. & Mantoura, R. (1997). Development of pigment methods for oceanography: SCOR-supported Working Groups and objectives In S. Jeffrey, R. Mantoura, & S. Wright (Eds.), *Phytoplankton pigments in oceanography: guidelines to modern methods* (pp. 19–36). Paris, France.: UNESCO Publishing.

Johnson, K.S., Chavez, F.P. & Friederich, G.E. (1999). Continental-shelf sediment as a primary source of iron for coastal phytoplankton. *Nature* 398(6729): 697. DOI: 10.1038/19511.

Khalil, I., Mannaerts, C. & Ambarwulan, W. (2009). Distribution of chlorophyll-a and sea surface temperature (SST) using modis data in east Kalimantan waters, Indonesia. *J. Sustain. Sci. Manage.* 4(2): 113–124.

Krishna, K.M. (2013). Cyclone Persuade on Chlorophyll-A Enrichment in the Bay of Bengal. *J. Geol. Geosci.* 2(134): 1–3. DOI: 10.4172/2329-6755.1000134.

Kuehl, S.A., Levy, B.M., Moore, W.S. & Allison, M.A. (1997). Subaqueous delta of the Ganges-Brahmaputra river system. *Mar. Geol.* 144(1–3): 81–96. DOI: 10.1016/s0025-3227(97)00075-3.

Levitus, S., Antonov, J.I., Wang, J., Delworth, T.L., Dixon, K.W. & Broccoli, A.J. (2001). Anthropogenic warming of Earth's climate system. *Science* 292(5515): 267–270. DOI: 10.1126/science.1058154.

Lorenzen, C.J. (1967). Determination of chlorophyll and pheo-pigments: spectrophotometric equations. *Limnol. Oceanogr.* 12(2): 343–346. DOI: 10.4319/lo.1967.12.2.0343.

Madhu, N., Maheswaran, P., Jyothibabu, R., Sunil, V., Revichandran, C. et al. (2002). Enhanced biological production off Chennai triggered by October 1999 super cyclone (Orissa). *Curr. Sci.* 82(12): 1472–1479. URL: http://drs.nio.org/drs/handle/2264/287.

Nagamani, P., Hussain, M., Choudhury, S., Panda, C., Sanghamitra, P. et al. (2013). Validation of chlorophyll-a algorithms in the coastal waters of Bay of Bengal initial validation results from OCM-2. *J. Indian Soc. Remote Sens.* 41(1): 117–125. DOI: 10.1007/s12524-012-0203-x.

Nagamani, P., Shikhakolli, R. & Chauhan, P. (2011). Phytoplankton variability in the Bay of Bengal during winter monsoon using Oceansat-1 Ocean Colour Monitor data. *J. Indian Soc. Remote Sens.* 39(1): 117–126. DOI: 10.1007/s12524-010-0056-0.

O'Reilly, J.E., Maritorena, S., Mitchell, B.G., Siegel, D.A., Carder, K.L. et al. (1998). Ocean color chlorophyll algorithms for SeaWiFS. J. *Geophys. Res.: Oceans* 103(C11): 24937–24953. DOI: 10.1029/98JC02160.

Patti, B., Guisande, C., Vergara, A., Riveiro, I., Maneiro, I. et al. (2008). Factors responsible for the differences in satellite-based chlorophyll a concentration between the major global upwelling areas. *Estuar. Coast. Shelf Sci.* 76(4): 775–786. DOI: 10.1016/j.ecss.2007.08.005

Poornima, D., Shanthi, R., Raja, S., Sethubathi, G.V., Thangaradjou, T. et al. (2013). Understanding the spatial variability of chlorophyll a and total suspended matter distribution along the southwest Bay of Bengal using in-situ and OCM-2 & MODIS-Aqua measurements. *J. Indian Soc. Remote Sens.* 41(3): 651–662. DOI: 10.1007/s12524-012-0233-4.

Prasad, A.K., & Singh, R.P. (2010). Chlorophyll, calcite, and suspended sediment concentrations in the Bay of Bengal and the Arabian Sea at the river mouths. *Adv. Space Res.* 45(1): 61–69. DOI: 10.1016/j.asr.2009.07.027.

Qasim, S. (1977). Biological productivity of the Indian Ocean. *Indian J. Mar. Sci.* 6(2): 122–137. URL: http://nopr.niscair.res.in/handle/123456789/39365.

Radiarta, I.N., & Saitoh, S.-I. (2008). Satellite-derived measurements of spatial and temporal chlorophyll-a variability in Funka Bay, southwestern Hokkaido, Japan. *Estuar. Coast. Shelf Sci.* 79(3): 400–408. DOI: 10.1016/j.

ecss.2008.04.017.

Sarangi, R. & Devi, K.N. (2017). Space-based observation of chlorophyll, sea surface temperature, nitrate, and sea surface height anomaly over the Bay of Bengal and Arabian Sea. *Adv. Space Res.* 59(1): 33–44. DOI: 10.1016/j.asr.2016.08.038.

Sarangi, R., Nayak, S. & Panigrahy, R. (2008). Monthly variability of chlorophyll and associated physical parameters in the southwest Bay of Bengal water using remote sensing data. *Indian J. Mar. Sci.* 37(3): 256–266. URL: http://hdl.handle.net/123456789/2047.

Sathyendranath, S., Gouveia, A.D., Shetye, S.R., Ravindran, P. & Platt, T. (1991). Biological control of surface temperature in the Arabian Sea. *Nature* 349(6304): 54. DOI: 10.1038/349054a0 .

Shetye, S., Gouveia, A., Shankar, D., Shenoi, S., Vinayachandran, P. et al. (1996). Hydrography and circulation in the western Bay of Bengal during the northeast monsoon. *J. Geophys. Res.: Oceans* 101(C6): 14011–14025. DOI: 10.1029/95jc03307.

Singh, R.P. & Chaturvedi, P. (2010). Comparison of chlorophyll concentration in the Bay of Bengal and the Arabian Sea using IRS-P4 OCM and MODIS Aqua. Indian *J. Geo-Mar. Sci.* 39(3): 334–340. URL: http://hdl.handle.net/123456789/10670.

Smyth, T.J., Miller, P.I., Groom, S.B. & Lavender, S.J. (2001). Remote sensing of sea surface temperature and chlorophyll during Lagrangian experiments at the Iberian margin. *Prog. Oceanogr.* 51(2–4), 269–281. DOI: 10.1016/S0079-6611(01)00070-2.

Subramaniam, A., Yager, P., Carpenter, E., Mahaffey, C., Björkman, K. et al. (2008). Amazon River enhances diazotrophy and carbon sequestration in the tropical North Atlantic Ocean. *Proc. Natl. Acad. Sci.* 105(30): 10460–10465. DOI: 10.1073/pnas.0710279105.

Suwannathatsa, S. & Wongwises, P. (2013). Chlorophyll distribution by oceanic model and satellite data in the Bay of Bengal and Andaman Sea. *Oceanol. Hydrobiol. Stud.* 42(2): 132–138. DOI: 10.2478/s13545-013-0066-y.

Venkateswrlu, P. & Rao, K. (2004). A study on cyclone induced productivity in South-Western Bay of Bengal during November-December 2000 using MODIS data products. In IGARSS 2004. 2004 IEEE International Geoscience and Remote Sensing Symposium, Anchorage, 20–24 Sept. 2004 (pp. 3496–3499). AK, USA: IEEE. DOI: 10.1109/IGARSS.2004.1370462.

Walton, C., Pichel, W., Sapper, J., & May, D. (1998). The development and operational application of nonlinear algorithms for the measurement of sea surface temperatures with the NOAA polar-orbiting environmental satellites. *J. Geophys. Res.: Oceans* 103(C12): 27999–28012. DOI: 10.1029/98JC02370.

Zhang, H., Qiu, Z., Sun, D., Wang, S. & He, Y. (2017). Seasonal and Interannual Variability of Satellite-Derived Chlorophyll-a (2000–2012) in the Bohai Sea, China. *Remote Sens.* 9(6): 582. DOI: 10.3390/rs9060582.